Influence of spin-orbit coupling on the transport and magnetic properties of Co_3Pd_{97}

P. A. Stampe, H. P. Kunkel, Z. Wang,* and G. Williams

Department of Physics, University of Manitoba, Winnipeg, Manitoba, Canada R3T 2N2

(Received 22 November 1994)

The influence of spin-orbit coupling on the transport and magnetic properties of Co_3Pd_{97} is investigated. Analysis of detailed field- and temperature-dependent ac susceptibility data yields a ferromagnetic ordering temperature of $T_C \simeq 137$ K, although asymptotic critical exponents describing this transition cannot be evaluated due to the presence of this coupling. This estimate for T_C is in excellent agreement with that deduced from the temperature derivative of the zero-field resistivity, from the temperature dependence of the coercive field, and from the temperature dependence of the low-field magnetoresistive anisotropy. The occurrence of this latter anisotropy relies on the presence of a spin-orbit interaction (with an associated orbital moment), and the behavior of this anistropy is compared with model calculations which incorporate this coupling.

INTRODUCTION

Multilayer films and superlattices based on Co and either Pd or Pt are of particular current interest due to their possible application in magneto-optic and magnetic recording processes.[1,2] Such usage results from the presence of a substantial magnetic anisotropy in a direction perpendicular to the multilayer structure, which in turn originates from the presence of an orbital component in the total moment at the Co site. Any such orbital moment (i.e., nonspherical charge distributions) possesses an orientationally dependent energy due to its interaction with the surrounding lattice electric ("crystal") field, and through the spin-orbit interaction this leads to an attendant angular dependent contribution from the total moment to the overall energy of the system, i.e., the so-called magnetocrystalline anisotropy. While this effect is relatively weak in metallic Co—a result attributed to an effective quenching of the orbital moment in this itinerant electron ferromagnet by the crystal field (the Co orbital moment amounts to only some 15% of the spin moment[3])—recent x-ray magnetic circular dichroism experiments have been interpreted as indicating a substantial enhancement of the "out-of-plane" Co orbital moment in these multilayer structures, an enhancement which correlates directly with increases in the associated first-order uniaxial anisotropy constant.[4]

Below we report the effects of the spin-orbit interaction on the magnetic and transport properties of bulk Pd+3 at. % Co. This composition, while considerably lower than that of the multilayer structures mentioned above, was chosen specifically to place the ferromagnetic ordering temperature in an accessible temperature range, thus enabling the influence of this interaction on the critical properties to be assessed. This assessment was done through detailed measurements of the field and temperature dependent ac susceptibility $\chi(H_a, T)$ for applied fields H_a in the range $0 \le \mu_0 H_a \le 0.1$ T in the vicinity of the Curie temperature $T_C \simeq 140$ K, and also included measurements of (i) the coercive field H_c (from butterfly loops $\chi(H_a, T)$ vs H_a at numerous fixed temperatures

$T \le T_C$); (ii) the zero-field resistivity $\rho(0, T)$ and its temperature derivative $d\rho/dT$ for $100 \le T \le 200$ K; (iii) the longitudinal $(\rho_\parallel)$ and transverse $(\rho_\perp)$ magnetoresistance at 4.2 K in applied fields $\mu_0 H_a$ to 2 T; and (iv) the low-field resistive anisotropy (LFRA) $[\rho_\parallel(H_a) - \rho_\perp(H_a)]$ in applied fields $\mu_0 H_a$ of 3, 6, 10, and 12.5 mT in the range of $120 \le T \le 150$ K. The existence of a difference between $\rho_\parallel$ and $\rho_\perp$ and, consequently, a LFRA depends upon the presence of an orbital moment and associated spin-orbit coupling. Indeed, the presence of an orbital moment at the Co site in this host was established initially a number of years ago from measurements of the spontaneous resistive anisotropy (SRA, i.e., the ratio $[\rho_\parallel(B) - \rho_\perp(B)]/\rho_\parallel(B)$ extrapolated to zero induction) and its variation with Co concentration;[5] such conclusions were confirmed by the analysis of subsequent Hall effect measurements.[6] However, while it is possible to understand the origin of such an orbital moment, at least in terms of an ionic based model[7] in which a $3d^7$ configuration is attributed to the Co site, the absence of such a moment in the case of Fe is more difficult to reconcile with the same model approach. Nevertheless, recent studies[8] of magnetic critical effects in PdFe of comparable composition provide a useful example of a system with no orbital moment/spin-orbit interaction, against which the present data will be contrasted.

EXPERIMENTAL DETAILS

A 5-g sample of nominal composition 3 at. % Co was prepared by arc melting high-purity Pd wire (5N's) and Co sheet (4N8). Homogeneity was ensured by inverting and remelting the resulting button five times, with negligible melting losses. This button was then severely plastically deformed by cold rolling it (between protective plastic strips) to form a sheet of thickness 0.15 mm from which specimens suitable for transport and magnetic measurements were cut. These samples were briefly etched (to remove possible surface contamination) before being annealed for 30 h at 1000 °C. While the high solubility of Co in Pd should ensure metallurgical homogenei-

ty in samples fast cooled from the melt, this later procedure of inverting then remelting followed by plastic deformation and subsequent annealing was adopted as a result of studies on this[9] and related systems[10−12] showing that it produced a high degree of homogeneity and a sharp magnetic transition.

The in-phase component of the susceptibility of a sample consisting of two (electrically insulated) strips, each with dimensions $(2 \times 0.3 \times 0.015)$ cm^3 (with rounded corners) was recorded continuously using a phase-locked susceptometer described previously,[13] with an ac driving field of 5 μT rms at 2.4 kHz applied along the largest specimen dimension. Static biasing fields $(\mu_0 H_a)$ up to 0.1 T were provided by a collinearly mounted solenoid and the temperature measured with a Au+0.03 at. % Fe versus Chromel P thermocouple. A specimen of dimensions $(4 \times 0.3 \times 0.015)$ cm^3, suitable for transport measurements, was mounted on a high-thermal-conductivity Cu block which could be inserted into a wide-bored (50 mm) superconducting solenoid. This block could be rotated through 90° about an axis perpendicular to that of the solenoid, so that the longitudinal and transverse magnetoresistance could be found at the same temperature (measured by a carbon-glass thermometer). The field-induced magnetoresistivity ratio $[\rho(H_a,T)-\rho(0,T)]/\rho(0,T)$ was measured with a precision approaching a few ppm using a low-frequency ac method[14] and the temperature derivative $d\rho/dT$ was estimated similarly from the ratio $[\rho(0,T+\Delta T)-\rho(0,T)]/\Delta T$ using temperature steps $\Delta T \sim 1$ K throughout the interval of interest. In both cases a current of about 50 mA was applied along the largest sample dimension. While this ac technique allows relative resistivity values to be determined with high precision, absolute resistivities have an estimated uncertainty approaching ±5% arising from a combination of shape factor and absolute ac voltage errors.

RESULTS AND DISCUSSION

A. ac susceptibility

Figure 1 reproduces measurements of the ac susceptibility $\chi(H_i,T)$ (corrected for background and demagnetizing effects) plotted against temperature in selected static biasing fields. In zero field $\chi(0,T)$ increases rapidly with decreasing temperature in the vicinity of the Curie temperature $T_C \simeq 137$ K, and while there is some structure in the response just below the principal (Hopkinson) maximum in $\chi(0,T)$—reminiscent of UFe$_2$[15]—the feature that should be stressed is that the magnitude of the susceptibility at this principal maximum is $\sim 3 \times 10^2$ J T^{-2} kg^{-1}, comparable to that reported for PdNi,[16] but much reduced from that observed in PdFe of comparable concentration[8] [where $\chi(0,T) \sim 2 \times 10^3$ J T^{-2} kg^{-1}]. Since all of these data were acquired in the same ac driving field from samples with essentially equal dimensions [for which the demagnetization factor N is consequently the same, although the demagnetization correction $(1-N\chi)^{-1}$ is roughly an order of magnitude larger (around 10–20 %) for samples containing Fe compared with those containing Co or Ni], and as these samples

were subjected to a similar annealing procedure (a procedure which is believed to enhance homogeneity), we suggest that this result provides indirect evidence that these differences arise from intrinsic (viz., orbital moments at the Co or Ni sites) rather than extrinsic (i.e., structural or metallurgical) sources.

The behavior of the susceptibility in nonzero superimposed fields supports this latter suggestion. As can also be seen from Fig. 1 these superimposed fields suppress the amplitude of the principal maximum and depress the temperature at which it occurs. This process enables the evolution of true critical peaks—reproduced in the inset in Fig. 1—to be resolved and followed. As discussed previously for a number of other systems[8,13,16−18] and in agreement with the behavior evident in this inset, the characteristics of these critical peaks are governed by the usual static scaling law appropriate to a paramagnetic to ferromagnetic transition,[19] and this indicates that the temperature T_m at which the critical peak occurs in-
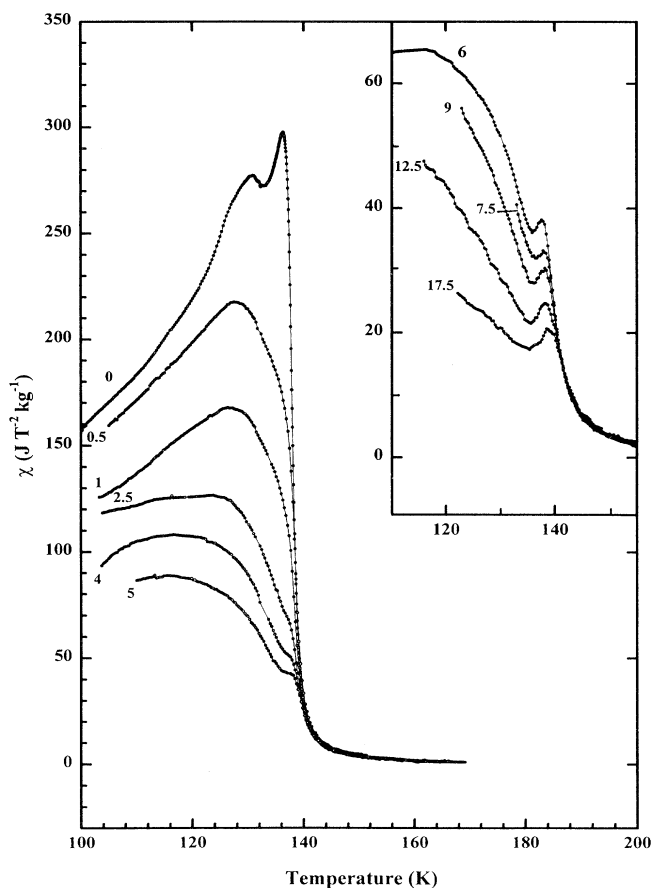
FIG. 1. The ac susceptibility (in J T^{-2} kg^{-1}), corrected for background and demagnetizing effects, plotted against temperature (in K) in the vicinity of the ferromagnetic ordering temperature. The numbers marked against each curve represent the superimposed static biasing fields (in mT). The inset summarizes the behavior in larger static biasing fields, which enables the evolution of the critical peaks to be followed.

creases with increasing field according to the power law

$$t_m = (T_m - T_C)/T_C \propto \left[\frac{H_i}{T_C} \right]^{1/(\gamma + \beta)} , \tag{1}$$

while the magnitude of the susceptibility at these critical maxima decreases with increasing field $h\,(\propto H_i/T_c)$, with

$$\chi(h, t_m) \propto h^{(1/\delta) - 1} . \tag{2}$$

A detailed discussion of the procedure followed to implement a self-consistent, systematic fit of Eqs. (1) and (2) to these data, along with the relationship between the zero-field susceptibility and reduced temperature t $[=(T - T_C)/T_C]$, i.e.,

$$\chi(0, t) \propto t^{-\gamma}, \quad T > T_C , \tag{3}$$

has been given on several previous occasions[8,13,16–18] and will not be reiterated here. However, what is important to stress is that these (secondary) critical maxima are a characteristic signature of critical fluctuations accompanying the phase transition, with the locus of the (secondary) critical maxima evident in the inset marking the boundary in the (h, t) plane of the so-called "crossover" line below which this critical response is field dominated but above which it is temperature dominated. By contrast the principal (Hopkinson) maximum is associated with the technical or regular components in the response (i.e., domain wall motion and/or coherent rotation, etc., and how the contribution from these components changes as the ratio of the coercive field to the ac driving field changes below T_C), not the singular/critical contribution. As is evident from Fig. 1, applied static fields $\mu_0 H_a$ in excess of about 6 mT are required to enable these technical contributions to be suppressed to a degree where the critical component dominates the measured (total) response; at lower fields this critical contribution appears as a shoulder on the $\chi(H, T)$ versus T plot (with no well-defined minimum at temperatures below the critical peak), while below 2.5 mT even this shoulder structure is obscured.

Systems in which the technical/regular contributions to the magnetization are not driven to saturation in low field are classified as magnetically hard; thus PdCo (and PdNi) contrasts markedly with soft systems such as PdFe in which the contribution from the singular/critical component dominates in fields as small as 0.1 mT.[8] We suggest that the most likely origin for this technical hardness in PdCo arises from single ion anisotropy at the Co site due to the presence of an orbital moment and spin-orbit coupling.

The occurrence of this technical hardness also complicates the analysis of the critical behavior of this system, precluding an accurate determination of the asymptotic critical exponents, as discussed below. Figure 2 reproduces a plot of the critical peak susceptibility (taken from data similar to that shown in the inset in Fig. 1) against the estimated internal field $\mu_0 H_i$ on a double logarithmic scale; this demonstrates clearly that a power law dependence [Eq. (2)] yielding a unique index δ is not obeyed by these data. The line drawn at lower fields in this figure
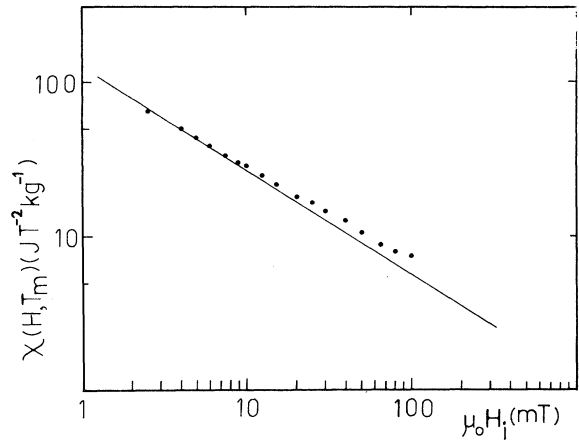
FIG. 2. The critical peak amplitude $\chi(H, T_m)$ (in J T^{-2} kg^{-1}) plotted against the estimated internal field $\mu_0 H_i$ (in mT) on a double logarithmic scale. The solid line yields an *effective* exponent ($\delta^* \simeq 3.1$) as discussed in the text.

corresponds to an *effective* exponent $\delta^*(H) \sim 3.1$ (close to the mean-field value but well below the value of $\delta = 4.8$ predicted by the localized, three-dimensional Heisenberg model[20]), while the curvature of the data themselves indicates that this effective exponent falls with increasing field. Effective $\delta^*(H)$ values which fall with increasing field have been reported in a number of other systems,[8,13,16] and its occurrence is consistent with the presence of considerable variance in the distribution of exchange coupling strengths (the couplings that lead to an ordered ground state); such a variance is expected in the present random alloy. The estimate of $\delta^*(H) \sim 3$ from the lower field data does *not* necessarily represent the true (asymptotic) value for this exponent, for two principal reasons: first, the resolution of critical peak structure is confined to fields in excess of 2.5 mT, well above that for "soft" systems, thus masking further possible increases in $\delta^*(H)$ as the $H \to 0$ asymptotic limit is approached; and second, it is very probable that there are substantial contributions from the residual (unsaturated) technical "background" to the peak amplitude plotted in Fig. 2, and this would invalidate the estimate obtained for $\delta^*(H)$ using Eq. (1) and the slope of Fig. 2. Similar considerations apply to Fig. 3, a double log plot of the (reduced) critical peak temperature against the internal field, i.e., a test of Eq. (1). Clearly this figure does not enable accurate values for the "crossover" exponent $(\gamma + \beta)$ to be established, again in contrast to the situation in "soft" systems; not only does this figure cover the same restricted field range as Fig. 1, but the error bars associated with the lower field points are also substantial. As discussed previously for PdNi,[16] such error bars reflect the large width (in temperature) of these critical peaks resulting from residual technical background contributions. These data thus do not rule out Heisenberg model exponents $(\gamma + \beta = 1.751[20])$, but then neither are mean-field exponents excluded $(\gamma + \beta = 1.5)$.

The behavior of the zero-field susceptibility is summa-
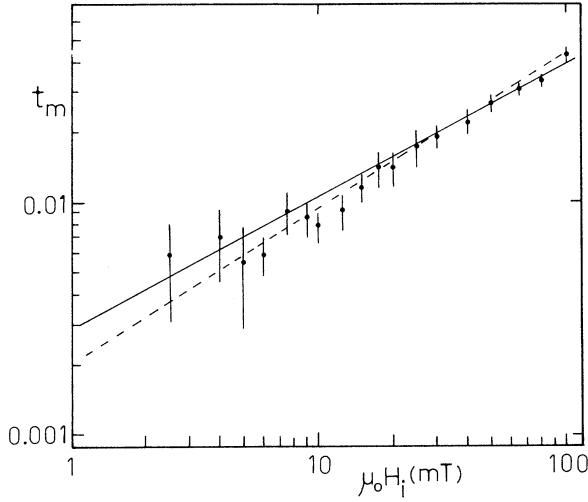
FIG. 3. The reduced critical peak temperature $t_m [=(T_m-T_C)/T_C$, with T_C taken as 136.8 K] plotted against the estimated internal field $\mu_0 H_i$ (in mT) on a double logarithmic scale. The solid line corresponds to 3D Heisenberg model exponents, and the dashed line to mean-field exponents.

rized in Fig. 4 by plotting the effective Kouvel-Fisher exponent[21]

$$\gamma^*(T) = d \ln(\chi(0,t))/d \ln(t) \qquad (4)$$

against t. The maximum in this effective exponent near $t \simeq 2 \times 10^{-2}$ confirms the presence of substantial exchange bond disorder[8,13,16-18,22] while the fall in $\gamma^*(T)$ below the Heisenberg model value of $\gamma = 1.386$ (Ref. 20) near $t \simeq 9 \times 10^{-3}$ simply reflects the result that $\chi(0,T)$ achieves only $\sim 1\%$ of its demagnetization factor limited value near T_C, as discussed earlier.

Summarizing, the field and temperature dependent susceptibility data near $T_C \simeq 136.8$ K exhibit a critical peak structure characteristic of critical fluctuation near a paramagnetic to ferromagnetic transition. However, the presence of a significant regular contribution to the measured response—reflecting the technically hard nature of this system—precludes the accurate evaluation of asymptotic critical exponents.
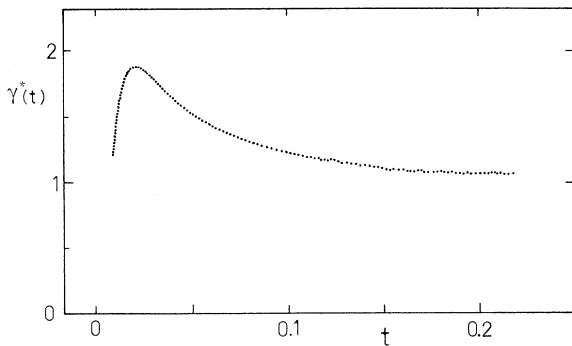
FIG. 4. The Kouvel-Fisher effective exponent $\gamma^*(t)$ plotted against reduced temperature t.

B. Coercivity

Figure 5 summarizes the temperature dependence of the coercive field $\mu_0 H_c$ estimated from the splitting between the maxima of plots of $\chi(H_a, T)$ vs H_a—so-called "butterfly loop"[8]—at various fixed temperatures $T \le T_c$. H_c vanishes at 137 ± 1 K, confirming the T_C estimate used in constructing Figs. 3 and 4. The magnitude of H_c increases quite rapidly below T_c, reaching a value of ~ 3 mT at $T_C/2$, about an order of magnitude larger than that recently reported from a related study of the $Fe_{10}Pt_{90}$ system.[18]

This relatively rapid increase in H_c below T_C correlates with the significantly larger technical component in the present system as indicated, for example, by the lowest field capable of resolving the critical peak structure.

C. Spontaneous resistive anisotropy (SRA)

The SRA, defined by the ratio[23]

$$\frac{\Delta\rho(B \to 0)}{\rho_0} = [\{\rho_\parallel(B) - \rho_\perp(B)\}/\rho_0]_{B \to 0} \qquad (5)$$

is estimated from Fig. 6, which reproduces the field-induced change in resistivity $\Delta\rho/\rho_0 = [\rho(H_a) - \rho(0)]/\rho(0)$ in the longitudinal ($\parallel$) and transverse ($\perp$) configurations in applied fields $\mu_0 H_a$ up to 2 T at 4.2 K. Beyond about 0.7 T, both $\rho_\parallel$ and $\rho_\perp$ display little dependence on field (ρ_0 is estimated at 3.7 ± 0.2 $\mu\Omega$ cm at this temperature), so that it is valid to estimate the SRA on an extrapolation based on H_a (rather than B), as is done in this figure. This yields SRA $\sim 1.7 \pm 0.05\%$, in good agreement with previous estimates.[5,24] The presence of spin-orbit coupling is a prerequisite for the observation of a magnetoresistive anisotropy, as discussed earlier. Figure 6 also shows that the average magnetoresistance

$$\rho(H_a, T) = [\rho_\parallel(H_a, T) + 2\rho_\perp(H_a, T)]/3 \qquad (6)$$

FIG. 5. The coercive field $\mu_0 H_c$ (in mT) plotted against temperature (in K).
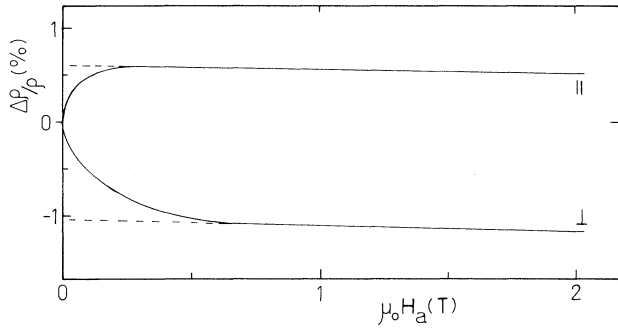
FIG. 6. The field-induced change in resistivity $\Delta\rho/\rho_0$ (in %) at 4.2 K plotted against the applied field $\mu_0 H_a$ (in T) for the longitudinal ($\parallel$) and transverse ($\perp$) configurations.

D. Resistivity and its temperature derivative

Figure 7 reproduces the zero-field resistivity $\rho(0,T)$ and its temperature derivative $d\rho/dT$ over the temperature interval 100–200 K, with the absolute values of these parameters being uncertain to typically $\pm 5\%$ as discussed previously.

The zero-field resistivity displays a distinct anomaly near T_C, best illustrated by its temperature derivative, the maximum in which is taken as defining T_C;[25] from Fig. 7, T_C is estimated at 136^{+1}_{-2} K (the errors arising from both scatter in the measured derivatives and absolute temperature uncertainties), in good agreement with the values derived from the analysis of the susceptibility data and the temperature dependence of the coercive field (using different thermometry).

From the lower section of Fig. 7 it can be seen that the measured values for $d\rho/dT$ (the $\pm 5\%$ uncertainty in absolute value notwithstanding) in this system decreases rapidly above 140 K, approaching a value of around 37 $n\Omega$ cm /K near 160 K, above which this derivative decreases slowly to a value near 35 $n\Omega$ cm /K at 190–200 K. While this decline in the magnitude of $d\rho/dT$ between 160 and 200 K is comparable to that reported in pure Pd, the absolute values for the derivative shown in Fig. 7 in this temperature range are typically ~ 5 $n\Omega$ cm /K smaller than those measured in the host metal.[26] Previous studies[26] have shown this to be a general feature of Pd-based alloys, which contrast in this respect with Pt-based systems where little change in $d\rho/dT$ from that of the undoped host is seen at higher temperatures.[18,26] As discussed recently for $Fe_{10}Pt_{90}$,[18] the persistence of enhanced values for $d\rho/dT$ at temperatures well above 136 K (in the present case, from around 136 K up to 155–160 K) is taken as indicating the existence of short-ranged spin correlations well above T_C in this system also. Correspondingly,[18] the resistivity measured near 160 K ($t \simeq 0.15$) is likely to be more representative

of that from the totally disordered state than the resistivity at T_c itself (although the temperature at which complete disorder is achieved is more difficult to estimate in the present system for the reasons indicated above). With this assignment, an estimate for the total magnetic component $\Delta\rho_m$ in the resistivity of this system (assuming the additivity of the various contributions) can be found using[18]

$$\Delta\rho_m \simeq [\rho(0,160 \text{ K})-\rho(0,4.2 \text{ K})]$$

$$-[\rho_{Pd}(160 \text{ K})-\rho_{Pd}(4.2 \text{ K})]$$

$$= 1.41 \ \mu\Omega \text{ cm} .$$

In terms of a localized s-d model in which this magnetic scattering arises from deviations of the lattice potential from ideal periodicity at the Co sites, with the scattering/perturbing potential including both a screened Coulomb (V) and a Pd conduction electron (σ)-Co spin (S) exchange term ($-2J\mathbf{S}\cdot\boldsymbol{\sigma}$), $\Delta\rho_m$ can be written as[27]

$$\Delta\rho_m \simeq AcJ^2S(1+4S) \tag{7}$$
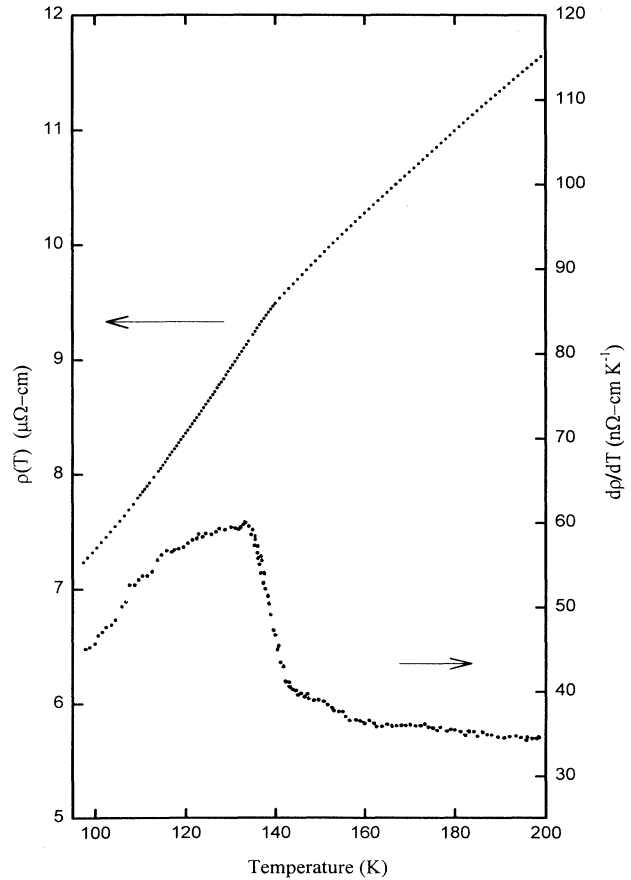
FIG. 7. The zero-field resistivity $\rho(T)$ (in $\mu\Omega$ cm) and its temperature derivative $d\rho/dT$ (in $n\Omega$ cm /K) plotted against temperature (in K). Note that while the relative values for these quantities can be determined with high precision, absolute values are uncertain to typically $\pm 5\%$, as discussed in the text.

is still negative at this temperature—despite the latter being a small fraction (~ 0.03) of T_C—decreasing by some 24 $n\Omega$ cm (0.55%) before saturating, again in good agreement with previous data.[24]

when $V^2 \gg J^2$. Here the factor A, given by

$$A = \frac{3\pi m^* \Omega}{2\hbar e^2 E_F}$$

depends on details of the band structure (the s-electron effective mass m^*, atomic volume Ω, and Fermi energy E_F), assuming a value of 6.56 $\mu\Omega$ cm at. $\%^{-1}$ eV^{-2} when c is the Co concentration in atomic percent and V and J (in reality, potential and exchange integrals averaged over the Fermi surface[28]) are in eV.[27] Estimates for the Co spin S can be obtained by combining saturation magnetization data[29] (measuring gS) with ferromagnetic resonance measurements[30] (yielding an impurity splitting factor of $g \simeq 2.4$), from which $S \simeq 3$ at this Co concentration. This yields for the local moment–s-electron exchange coupling

$$|J| \simeq 0.043 \text{ eV} ,$$

in reasonably good agreement with values estimated from earlier resistivity measurements [0.047–0.066 eV (Ref. 31)] on alloys of comparable concentration.

Finally, from $\rho(0,4.2$ K) it is possible, using s-d model expressions, to verify the validity of the inequality used above, viz., $V^2 \gg J^2$. Assuming that the ground state is completely ordered at 4.2 K [a reasonable approximation since, while there is a field-induced negative (average) magnetoresistance at this temperature, it represents only some $\sim \frac{1}{2}\%$], then

$$\rho(0,4.2 \text{ K}) \simeq Ac[V^2 - 3J^2S^2] , \tag{8}$$

from which $|V| \simeq 0.49$ eV, justifying the above assumption.

E. Low-field resistive anisotropy (LFRA)

Measurements of the LFRA, that is, of the ratio

$$\frac{\Delta\rho(H_a,T)}{\rho(0,T)} = [\rho_\parallel(H_a,T) - \rho_\perp(H_a,T)]/\rho_\parallel(H_a,T) \tag{9}$$

at various fixed temperatures in the interval $100 \leq T < 150$ K in applied fields of 3, 6, 10, and 12.5 mT are reproduced in Fig. 8. The line drawn through these data close to T_C indicates (i) that this anisotropy vanishes at 137±1 K, providing another estimate for T_c (and in good agreement with those found above) and (ii) that within experimental uncertainty, these data, collected in different applied fields, collapse onto a single line as T_C is approached from below, in agreement with itinerant and localized model predictions. In terms of either model approach, as discussed in detail recently,[18] the presence of a magnetoresistive anisotropy relies on two essential ingredients: (a) an orbital component (and hence spin-orbit coupling λL·S) at scattering sites and (b) a polarizing field.

In itinerant model approaches [based on Mott's two-current model,[31] i.e., parallel conduction in spin-up (+) and spin-down (−) subbands] to systems like PdCo, in which the conductivity is s-electron dominated while the magnetic properties are determined principally by the d-electron response, the resistive anisotropy in low applied
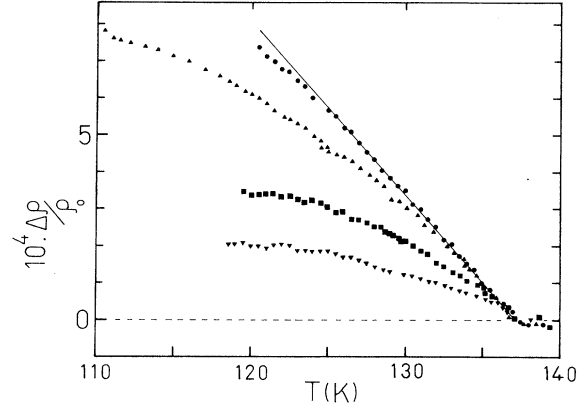
FIG. 8. The low-field resistive anisotropy (LFRA) $\Delta\rho/\rho$ measured in applied fields $\mu_0 H_a$ of 3 (▼), 6 (■), 10 (▲), and 12.5 (●) mT, plotted against temperature (in K).

fields can be expressed as[18]

$$\frac{\Delta\rho}{\rho} \propto \frac{(\lambda/K)^2(dN/dE)^2_{E_F}(T - T_c)}{\rho_+\rho_- + \rho_\pm(\rho_+ + \rho_-)} . \tag{10}$$

Here $\rho_\pm$ arises from interband scattering,[32] and K measures the splitting induced by a cubic anisotropy[33] (which must be included if problems in the predicted behavior of the LFRA at T_c —where the exchange field collapses— are to be avoided). The term involving $(dN/dE)_{E_F}$ —the density of states near the Fermi energy E_F —originates from an expansion of the subband resistivity in terms of the exchange field H_{ex},[18,33] and the linear dependence $(T - T_C)$ reflects the temperature dependence of H^2_{ex} in conventional band theory.[18,34] Thus the vanishing of the LFRA at T_C (mentioned above) confirms that the polarizing field in the present experiment is in fact the exchange field, with (small) applied fields simply enabling a domain size to be established on a length scale comparable to the electronic mean-free path. While similar conclusions are reached by localized models, the presence of small external fields in them serves the additional function of defining a quantization axis for spin-orbit coupling; thus the alignment of the spin dipole moment (S) by the polarizing exchange field also results (via the spin-orbit interaction) in an attendant orientation of the orbital moment (L) and hence the associated nonspherical charge distribution. A multipole analysis of this latter distribution indicates that the leading contribution to the asymmetry in the field dependent resistivity arises from electric quadrupole (D) scattering[31,35,18], with

$$\frac{\Delta\rho}{\rho} \simeq \left[\frac{D}{V}\right][\langle S_z^2 \rangle_T - S(S+1)/3] . \tag{11}$$

The obvious advantage of this localized model expression is that it does not involve details of the band structure, unlike (10) (although the ratio of the coupling constants D/V, which determine the sign of $\Delta\rho$, remains to be specified). The behavior of the temperature and field dependence of the LFRA have been obtained using Eq.
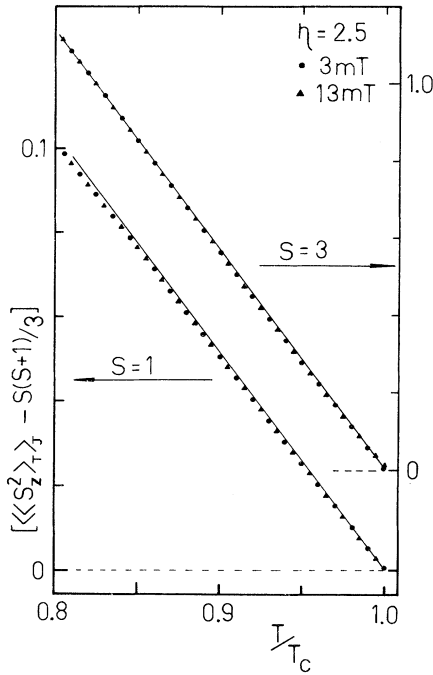
FIG. 9. The calculated quadrupolar term $\langle\langle S_Z^2\rangle_T\rangle_J$ $-S(S+1)/3$ (in arbitrary units) plotted against the reduced temperature T/T_C for spin values of $S=3$ and $S=1$, with $\eta=2.5$. The symbols correspond to the applied field values shown when T_C is taken as 140 K.

(11) in conjunction with an effective field Ising Hamiltonian[36] incorporating both a Gaussian distribution of exchange coupling strengths between the Co spins and a uniform external field. In this particular localized model the thermal average ($\langle\ \rangle_T$) involved in the quadrupolar term appearing in Eq. (11) is replaced by a double average $\langle\langle S_Z^2\rangle_T\rangle_J$ over both temperature and exchange. The results of this calculation are presented in Fig. 9 using applied fields which cover the range used experimentally (the calculation incorporates a spin of $S=3$ as discussed above, and assumes a value of 2.5 for the ratio $\eta=\bar{J}_0/\bar{J}$ of the first to second moment of the Gaussian exchange bond distribution; the choice $\eta>1.25$ is dictated by the appearance of a ferromagnetic ground state[37,38]; these calculations suggest that over the range covered, the LFRA should display a field independent linear decrease above about 120 K. A similar result (although over an unspecified applied field range) would also be predicted by the itinerant model expression—Eq. (10)—*provided the temperature dependence of the anisotropy was dominated by the temperature dependence of the exchange field* (at least in mean field). However, in either model approach it is important to emphasize that a nonzero LFRA only occurs in the presence of spin-orbit coupling (i.e., $\lambda\neq0$, with L, and hence D, also nonzero).

In contrast with the model predictions shown in Fig. 9, the experimental data, while approaching a field independent linear decrease close to T_C, do so only above about 133 K (i.e., much closer to T_C); while the deviation of the LFRA from a simple linear increase, evident in the model calculations reproduced in Fig. 9, are dependent (for a

specified applied field range) on the values adopted for both S and η, this dependence is generally much weaker than that observed in the present experiment. Problems can arise as $\eta\rightarrow1.25$ and the limit of stability of the ferromagnetic ground state is approached,[37,38] available data do not suggest that Co_3Pd_{97} is close to this instability. As in the case of $Fe_{10}Pt_{90}$,[18] we reiterate that these models approaches do *not* include domain effects, and suggest that the deviations observed in the experimental data are due to the inability of the lower applied fields utilized to render the system single domain over the length scales probed in these experiments.

SUMMARY AND CONCLUSIONS

The analysis of detailed transport and magnetic measurements on Co_3Pd_{97} reveals a marked influence of the spin-orbit interaction. The ac susceptibility data display features characteristic of critical fluctuations accompanying a paramagnetic to ferromagnetic transition, but while these critical peak data yield an estimate for T_C of 137 ± 1 K, values for the asymptotic critical exponents cannot be found due to the presence of anisotropy—most likely originating from spin-orbit coupling. The above estimate for T_C is in good agreement with that found from the zero-field resistivity (viz., from the temperature of the maximum in $d\rho/dT$) and from the temperature at which the LFRA vanishes. The temperature dependence of the LFRA immediately below T_C is also in agreement with model predictions, although the measured anisotropy falls well below the model value as the temperature is decreased further. This latter difference is attributed to the influence of domain structure, the model calculations being valid only within a single domain. The presence of both a LFRA and a SRA confirms the presence of spin-orbit coupling.

Finally, it is interesting to compare and contrast the behavior of the LFRA near T_C in Co_3Pd_{97} with that in $Fe_{10}Pt_{90}$. In both systems differences between model predictions and experimental data occur immediately below T_C in the lowest measuring field (~3 mT), despite the result that this measuring field far exceeds the coercive field H_c at these temperature. However, at a given interval ΔT ($=T_C-T$) below T_C, while both the electronic mean-free path (MFP) (at least as judged from the resistivity) and the coercive field in PdCo exceed those in PtFe, deviations from the model predicted behavior are observed *closer* to T_C in the latter system, contrary to the behavior expected from both H_c, and the MFP. This result would *seem* to indicate a much larger domain size in Co_3Pd_{97} despite its larger H_c, although the magnetoresistive anisotropy measured in the lowest fields does appear to saturate more quickly in PdCo than in PtFe. We are currently attempting to validate this inference regarding domain size using more direct techniques.

ACKNOWLEDGMENTS

*Present address: Department of Physics, Dalhousie University, Halifax, Nova Scotia, Canada B3H 3J5.

[1]T. Suzuki, M. Ozkan, and D. Dobbertin, Acta Metall. (to be published).

[2]T. Kingetsu, J. Magn. Magn. Mater. **135**, 303 (1994).

[3]R. A. Reck and D. L. Fry, Phys. Rev. **184**, 492 (1969).

[4]D. Weller, Y. Wu, J. Stöhr, M. G. Samant, B. D. Hermsmeier, and C. Chappert, Phys. Rev. B **49**, 12 888 (1994).

[5]S. Senoussi, I. A. Campbell, and A. Fert, Solid State Commun. **21**, 269 (1977).

[6]A. Hamzić, S. Senoussi, I. A. Campbell, and A. Fert, Solid State Commun. **26**, 617 (1978).

[7]L. L. Hirst, Phys. Condens. Matter **11**, 255 (1970).

[8]Z. Wang, H. P. Kunkel, and G. Williams, J. Phys. Condens. Matter **4**, 10 385 (1992).

[9]A. Pilipowiez and H. Claus, Phys. Rev. B **36**, 773 (1987).

[10]S. Crane, D. W. Carnegie, and H. Claus, J. Appl. Phys. **53**, 2179 (1982).

[11]J. Ododo, J. Phys. F **9**, 1441 (1979).

[12]C. Buscher, T. Auerswald, E. Scheer, A. Schröder, H. V. Lohneysen, and H. Claus, Phys. Rev. B **46**, 983 (1992).

[13]I. Maartense, Rev. Sci. Instrum. **41**, 657 (1970); G. Williams, in *Magnetic Susceptibility of Superconductors and Other Spin Systems,* edited by R. A. Hein *et al.* (Plenum, New York, 1991), p. 475 ff.

[14]W. B. Muir and J. O. Ström-Olsen, J. Phys. E **9**, 163 (1976).

[15]H. P. Kunkel, J. M. Schachter, and G. Williams, *International Conference on the Physics of Transition Metals,* edited by P. M. Oppeneer and J. Kübler (World Scientific, Singapore, 1993), p. 855; S. B. Roy, G. Williams, and B. R. Coles, J. Phys. (Paris) **50**, 2773 (1989).

[16]Z. Wang, H. P. Kunkel, and G. Williams, J. Phys. Condens. Matter **2**, 4173 (1990).

[17]H. Ma, H. P. Kunkel, and G. Williams, J. Phys. Condens. Matter **3**, 5563 (1991).

[18]P. A. Stampe, X. Chen, Z. Wang, H. P. Kunkel, and G. Williams, J. Phys. Condens. Matter **6**, 3045 (1994).

[19]H. E. Stanley, *Introduction to Phase Transitions and Critical Phenomena* (Clarendon, Oxford, 1971).

[20]L. C. LeGuillou and J. Zinn-Justin, Phys. Rev. B **21**, 3976 (1980).

[21]J. S. Kouvel and M. E. Fisher, Phys. Rev. A **136**, 1626 (1964).

[22]S. N. Kaul, J. Magn. Magn. Mater. **53**, 5 (1985).

[23]J. W. F. Dorleijn, Philips Res. Rep. **31**, 287 (1976).

[24]A. Hamzić, S. Senoussi, I. A. Campbell, and A. Fert, J. Phys. F **8**, 1947 (1978).

[25]J. A. Mydosh, J. I. Budnick, M. P. Kawatra, and S. Skalski, Phys. Rev. Lett. **21**, 1346 (1968); M. P. Kawatra and J. I. Budnick, Int. J. Magn. **1**, 61 (1970).

[26]J. Bass, in *Metals: Electronic Transport Phenomena,* edited by K.-H. Hellwege and J. L. Olsen, Landolt Börnstein, New Series, Group 3, Vol. 15, Pt. a (Springer-Verlag, Berlin, 1982), p. 1.

[27]J. Bews, A. W. Sheikh, and G. Williams, J. Phys. F **16**, 1537 (1986); R. N. Kleiman and G. Williams, *ibid.* **12**, 169 (1982).

[28]K. Yosida, Phys. Rev. **107**, 396 (1957).

[29]R. M. Bozorth, P. A. Wolff, D. D. Davis, V. B. Compton, and J. H. Wernick, Phys. Rev. **122**, 1157 (1961).

[30]D. N. S. Bagguley, W. A. Crossley, and J. Liesegang, Proc. Phys. Soc. London **90**, 1047 (1967).

[31]N. F. Mott, Proc. R. Soc. A **153**, 699 (1936); I. A. Campbell and A. Fert, *Ferromagnetic Materials,* edited by E. P. Wohlfarth (North-Holland, Amsterdam, 1982), Vol. 3, p. 747 ff.

[32]I. A. Campbell, A. Fert, and O. Jaoul, J. Phys. C **3**, S595 (1970).

[33]A. P. Malozemoff, Phys. Rev. B **34**, 1853 (1986).

[34]A. H. Wilson, *The Theory of Metals* (Cambridge Univ. Press, Cambridge, 1965).

[35]A. Freiderich and A. Fert, Phys. Rev. Lett. **33**, 1214 (1972).

[36]T. Kaneyoshi, J. Phys. C **8**, 3415 (1975); B. W. Southern, *ibid.* **9**, 4011 (1976).

[37]R. M. Roshko and G. Williams, J. Phys. F **14**, 703 (1984).

[38]P. A. Stampe, H. P. Kunkel, and G. Williams, J. Phys. Condens. Matter **5**, L625 (1993).